54

HUMAN INDUCED INSTABILITY IN HAPTIC INTERFACES

H. Kazerooni
Department of Mechanical Engineering
University of California
Berkeley, California

ABSTACT

Powered hand controllers are active multi-degree-of-freedom joystick-like mechanisms which are maneuvered by humans to generate commands. They can be used as force reflecting master robots in telerobotic systems. Powered hand controllers can also be used by helicopter pilots for commanding pitch and roll. Another application involves maneuvering unmanned underwater vehicles where the operator maneuvers the vehicle from a mother ship using a hand controller.

This article describes the dynamic behavior of a hand controller when it is maneuvered by a human. A general control architecture is developed which guarentees various impedences on the hand controller. We show that some compliancy either in the hand controller or in the human arm is necessary to achieve stability of the hand controller and the human arm taken as a whole. The actuators' backdrivability, the dynamics of the hand controller mechanisms, and the computer sampling time are discussed as they relate to system stability.

A set of experiments which were performed on a prototype hand controller are presented to show the system performance.

NOMENCLATURE[1]

$E(s)$	the dynamics of the hand controller mechanism, s is the Laplace variable
$e(s)$	input command to the hand controller
$f(s)$	force on the hand controller
$G(s)$	hand controller dynamics with positioning controller
$H(s)$	human arm dynamics
$K(s)$	compensator (operating on the contact force, f)
K_o	DC gain of $K(s)$
τ	time constant of $K(s)$
$x(s)$	hand controller position

[1] The Laplace argument, s, for all functions will be omitted throughout this article except when new quantities are defined or when required for clarity.

1. INTRODUCTION

Hand controllers are multi-degree-of-freedom mechanisms which are used to command a variety of machines including, robotic systems, helicopters, and underwater and space vehicles. Figure 1 shows a multi-degree-of-freedom hand controller being maneuvered by a human. Hand controllers should be discriminated from controllers which consist of multiple levers and switches. A hand controller allows multiple commands to be integrated into a single hand movement. The novelty of hand controllers is apparent in manauvering unmanned underwater vehicles. (Traditionally, the speed of the underwater vehicle in various directions is a function of the position of the hand controller in various directions.) The operator can control the three dimensional motion of the vehicle from a single handgrip.

Hand controllers fall into two categories: passive and active. Passive hand controllers are not powered and do not provide any force feedback to the operator. The passive hand controller consists of linkages, encoders and other passive elements. Some passive handcontrollers also include springs and dampers in the joints to provide resistance to motion. Reference [13] describes a multi-degree-of-freedom passive hand controller used for helicopter flight control. Reference [6] formulates a helicopter handling quality using a multi-degree-freedom passive hand controller. A fundamental limitation in performance of passive hand controller arises from the operator inability to modulate the hand controller dynamic behavior. This is true because the passive hand controller's behavior is a fixed function of the mechanism dynamics. Active hand controllers, however, include powered actuators in the mechanism joints. The actuator at each joint is used to produce an arbitrary resistance to the operator's motion. This resistance to motion can be modulated to provide different dynamics in different directions. For example, since the human arm is stronger in a pitch motion than a roll motion, pilots usually prefer to feel a large stiffness in the pitch

motion and a small stiffness in the roll motion. In another example, the hand controller may have to be rolled and pitched along arbirary pivots that are not located at the same point. Note that the axes of the coordinate frame for a desired dynamic behavior (impedances), in general, do not coincide with the hand controller's motors' axes; these desired impedances must be developed electronically. See references [4 and 12] for description of two novel powered hand controllers.

Powered hand controllers are of paramount importance in force reflecting systems [14, 17]. In these systems, the hand controllers resistance to motion is a function of the forces applied to the controlled machine. For example, in manuevering an unmanned underwater vehicle with a force reflecting handcontroller, the position of the handcontroller would correspond to the velocity of the vehicle and the force on the handcontroller would correspond to the drag forces on the vehicle. In another example, a force reflecting handcontroller is the master in a master-slave telerobotic system. "Telepresence" denotes a dynamic behavior in telerobotic systems in which the environmental effects experienced by the slave are transferred through the master to the operator without alteration; therefore, the human feels that he/she is "there" without "being" there. See references [1, 2, 5, 18] for the role of force reflection in telemanipulations.

This article is concerned with the stability of a powered hand controller interacting with a human arm. In particular, the following topics are discussed in this paper:
1) Theoretical derivation of a control law that guarantees various impedances on the hand controller.
2) Derivation of the trade-offs between the achievable bandwidth and the desired impedance; one cannot choose an arbitrary soft impedance for the hand controller for a wide bandwidth.

Section 2 describes the hand controller and human arm dynamic behavior. Section 3 introduces the control architecture. Section 4

derives a stability condition. Section 5 gives some suggestion to prevent instability and finally Section 6 describes the trade-offs between the stability and performance via a set of experiments.
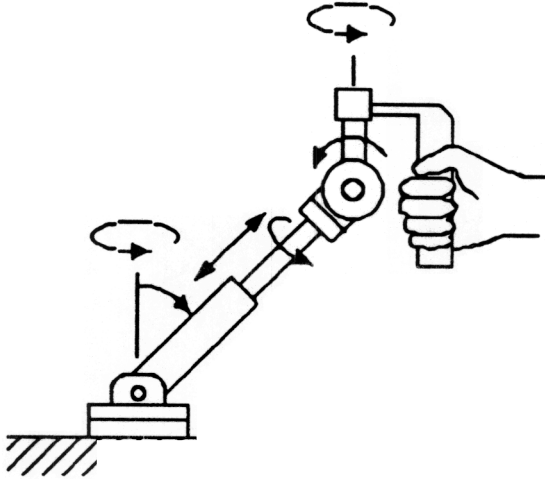

Figure 1: Schematic of as Six-Degree-of-Freedom Hand Controller

2. MODELING

This section models the dynamic behavior of the hand controller and the human arm. We represent the hand controller and human with general unstructured models. Since these models do not have a particular structure, they encompass a wide variety of hand controller and human arm dynamic behavior. Although this modeling approach may not lead to any design procedure, it will enable us to understand the fundamental issues in stability of a hand controller and human arm taken as a whole.

Hand Controller

The hand controller is assumed to have a closed-loop position controller. A closed-loop position control system minimizes the effects of frictional forces in the joints and in the transmission mechanism, and creates a more definite dynamic behavior in the mechanism. Minimizing the effects of uncertainty in electromechanical systems is a usual design specification for position controllers. (See

reference [15] for a design method). A closed-loop position control system creates linear dynamic behavior in the hand controller. Here it is assumed that, for non-linear hand controller dynamics, a nonlinear stabilizing controller has been designed to yield a nearly linear closed-loop position system for the hand controller. This lets us assume that the hand controller closed-loop dynamics can be approximated by transfer functions.

The end-point position of the hand controller is a dynamic function of both its input command, e, and the human force, f. The structure of the positioning controller is not of importance in this analysis. G and S are two transfer functions that relate the hand controller end-point position, x, to the input command, e, and the human force, f.

$$x = G e + S f \qquad (1)$$

The motion of the hand controller end-point in response to imposed forces (f) is caused by either structural compliance in the hand controller or by the compliance of the positioning controller. S is called the sensitivity function, and it maps the external forces to the hand controller position. Whenever an external force is applied to the hand controller, the end-point of the hand controller will move in response. If the hand controller has a "good" positioning controller, the change in position due to the external force will be "small" as long as the magnitude of the external force lies within certain limits. Note that G and S depend on the nature of the closed loop controller. If a compensator with several integrators is chosen to insure small steady state errors, then S will be small in comparison to G. If the hand controller actuators are non-backdrivable, then S will be small regardless of how carefully the hand controller's positioning compensator is chosen[2].

---

[2]Throughout this paper, we analyze hand controller and human arm dynamics using unstructured dynamic models which focus on the input-output relationships rather than a particular dynamic structure. The

Human Arm Dynamics

Human arm maneuvers fall into two categories: *unconstrained* and *constrained*. In unconstrained maneuvers, the human arm is not in contact with any object, while, in constrained maneuvers, the human arm is in contact with an object continuously. Since the human arm maneuvering the hand controller is always holding the hand controller, our primary focus is on constrained maneuvers of the human arm.

The force imposed by the human arm on the hand controller results from two inputs. The first input, m, is the force imposed by the human muscles[3], the second input is the motion of the hand controller. If the hand controller is stationary, the force imposed on the hand controller is a function only of muscle forces. However, if the hand controller moves, the force imposed on the hand controller is a function not only of the muscle forces but also of the motion of the hand controller. In other words, the human contact force with the hand controller will be disturbed and will be different from m, if the hand controller is in motion. H is defined in equation 2 to map the hand controller position, x, onto the contact force, f.

$$f = m - H x \qquad (2)$$

H is the human arm impedance and is determined primarily by the physical

---

framework of unstructured models leads to general conclusions, however a given hand controller's dynamics are typically characterized by a structured model

[3] It is assumed that the specified form of m is not known other than that it is the result of human thought deciding to impose a force onto the hand controller. The dynamic behavior in the generation of m by the human central nervous system is of little importance in this analysis since it does not affect the system performance and stability. See references [3, 7] for a description on the muscle dynamics.

properties of the human arm. This model is in agreement with the modeling described in Reference [16]. Figure 2 depicts how the hand controller and human interact dynamically.
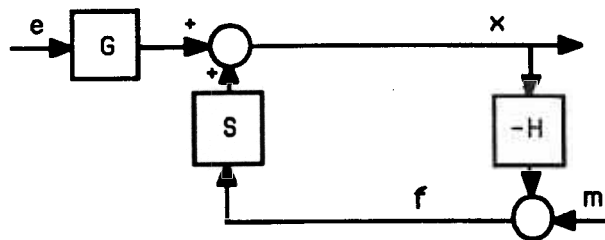

Figure 2: The Block Diagram of the Hand Controller and Human Arm.

3. THE CONTROL ARCHITECTURE

Figure 3 shows the system when force compensator, , is incorporated in the control structure. When the hand controller is not in contact with the human, the actual position of the hand controller end-point is governed by equation 1, where f = 0. The feedback loop on the contact force f closes naturally when the hand controller encounters the human arm. Examining figure 3 reveals that K provides additional paths for f to map to x. The physical contact between the human and the hand controller produces some hand controller motion as f acts through S. In general, S is small: thus, the human operator alone does not have sufficient strength to move the hand controller as desired. An additional route for f to map to x can be added if K is chosen to be non-zero; K can be thought of as the component that shapes the overall mapping of the force f to the position x. This leads to an effective sensitivity of (S + G K). (For brevity, we refer to the SH loop as the natural loop and the GKH loop as the compliance loop because it contains the compliance compensator, K)

G and S are fixed by the mechanical design of the hand controller and by the chosen position controller. The designer has some freedom (limited by stability considerations) to adjust the effective sensitivity (S + G K) along the path from f to x; (S + G K) affects how the hand controller "feels" to the human operator.

For instance, if K is chosen so (S + G K) is approximately a constant, the hand controller reacts like a spring in response to f. Similarly, if (S + G K) is approximately a single or double integrator, the hand controller acts like a damper or mass, respectively. A large value for K develops a compliant hand controller while a small K generates a stiff hand controller. One cannot choose arbitrarily large values for K; the stability of the closed-loop system of Figure 3 must also be guaranteed.
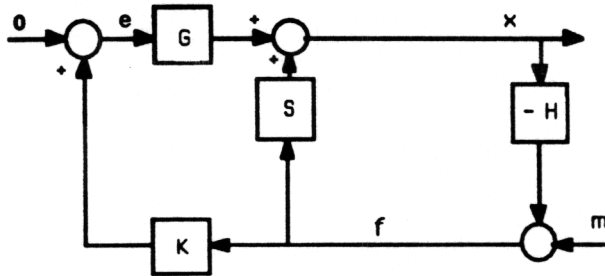

Figure 3: Addition of a Force Compensator to the Hand Controller

4. THE CLOSED-LOOP STABILITY CONDITION

The Nyquist Theorem is used to develope a sufficient stability condition for the closed-loop system in Figure 3. This sufficient condition results in a class of compensator K which guarantees the stability of the closed-loop system. Note that the stability condition derived in this section does not give any indication of system performance, but only ensures a stable system. Also, note that the stability condition is a sufficient condition not a necessary condition.

An assumption is made that the system in Figure 3 is stable when K = 0. The plan is to determine how robust the system is when the term (GKH) is added to the feedback loop. Note that there are two elements in the feedback loop: S H represents the natural feedback loops which occur as a result of the interaction between the human arm and the hand controller while G K H represents the controlled feedback loops. If the controller in

the feedback loop is eliminated by setting K = 0, the system reduces to the case where a human is manipulating the hand controller, but the command input to the hand controller closed-loop position system is zero. The goal is to obtain a sufficient stability condition when K is added to the system. To achieve this, the Nyquist criterion [11] is used. The following assumptions are made:

1. The closed-loop system in Figure 3 is stable when K = 0. It is assumed that the system remains stable when the human and the hand controller are in contact and no feedback is used in the system.
2. K is chosen as stable linear transfer function. Therefore the loop transfer function, (S H + G K H), has the same number of right half-plane poles as (S H). For convenience in stability analysis we assume A = (S H) and B = (S H + G K H).

According to the Nyquist criterion, the system shown in Figure 3 remains stable as long as the number of anti-clockwise encirclements of B around the origin of the s-plane is equal to the number of unstable poles of the loop transfer function, B. By assumptions 1 and 2, A and B have the same number of unstable poles. Assuming that the system is stable when K = 0, the number of encirclements of the origin by (1 + A) is equal to the number of unstable poles in A. When compensator K is added to the system, the number of encirclements of the origin by (1 + B) must be equal to the number of unstable poles in B in order to guarantee closed-loop stability. Because of the assumption that the number of unstable poles in A and B are identical, (1 + B) must have exactly the same number of encirclements of the origin as (1 + A). In order to guarantee equal encirclements by (1 + B) and (1 + A), insurance is needed so that (1 + B) does not pass through the origin of the s-plane for all frequencies.

$$+ S H + G K H | \neq 0 \quad \forall \omega \in (0, \infty) \quad (3)$$

A more conservative condition can be written as:

$$|GKH| < |1+SH| \quad \forall \omega \in [0, \infty) \quad (4)$$

Or:

$$|GK| < |S + 1/H| \quad \forall \omega \in [0, \infty) \quad (5)$$

Inequalities 4 and 5 express the stability condition of the closed-loop system in Figure 3 [4]. Inspection of inequalities 4 and 5 show that the smaller the sensitivity of the hand controller, the smaller K must be. Also from inequality 5, the more rigid the human arm is, the smaller K must be. In the "limiting case" when the hand controller is infinitely stiff $(S = 0)$, no K can be found to enable interaction with an infinitely rigid human arm $(H \rightarrow \infty)$. In other words, for stability of the system shown in Figure 3, there must be some compliancy either in the hand controller or in the human arm. The hand controller compliancy may be due to structural flexibility, and/or the electronic compliancy resulting from the positioning controller.

The stability condition for multi-degree-of-freedom (when G, K, H, and S are transfer function matrices) can be derived in a similar way using singular values.

$$\sigma_{max}(GKH) < \sigma_{min}(I + SH)$$
$$\forall \omega \in [0, \infty) \quad (6)$$

The next section gives some suggestions to increase the system stability range:

---

[4] A less conservative stability condition to guarantee inequality is:

The angle of $(GHK + SH) < 180$

$$\forall \omega \in [0, \infty)$$

whenever $|GHK + SH| = 1$

The above inequality states that guaranteeing stability of the closed-loop system requires selecting K such that the phase margin for the loop gain of $(GHK + SH)$ is positive.

5. SUGGESTIONS TO INCREASE THE STABILITY RANGE

1) Increasing the Sensitivity Function

Transmission systems with large transmission ratios are not backdrivable and result in small sensitivity functions (S). We suggest that the hand controllers be designed to be backdrivable. This can be done by employing low-ratio transmission systems to drive the hand controller. Direct drive systems, because of the elimination of the transmission systems, can potentially have large S. Appendix A shows how to choose a transmission ratio that yields the maximum acceleration for the hand controller.

Another method of increasing S is to decrease the position controller gain. The decrease in the position control gain may result in a sluggish response for the hand controller. However, we suggest that this gain be chosen to be as small as possible. In particular, we recommend that integral control must be avoided in the position control loop. Integrators in the position loop result in a very small S, even in the presence of backdrivable actuators.

2) Mechanism Dynamics

The more rigid the structure of the hand controller is, the wider the achievable bandwidth of G is. A hand controller, which has too many mechanical elements bolted together, will have dynamics that cannot be modeled correctly. If the hand controller mechanism is very rigid, then the block diagram of Figure 3 is correct. However, if the mechanism contains large unmodeled dynamics, the block diagram of Figure 4 is more appropriate. E represents the structural dynamics associated with the flexibilities in the hand controller mechanism

Note that loop SH is not an "information" loop; it is a "power" loop. This loop shows how the human force affects the hand controller. The force imposed by the human may have frequency components that

will excite the unmodelled structural modes of the system represented by E which will be read by the force sensor.
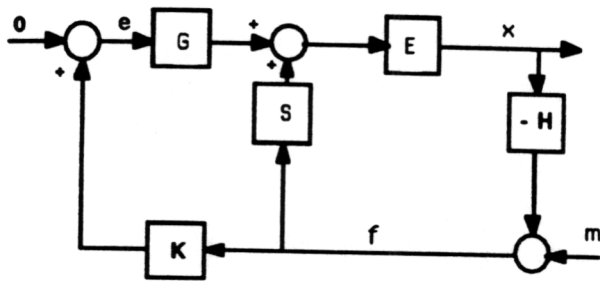

Figure 4: Addition of the
Mechanism Dynamics, E.

Using the Nyquist stability criteria, the stability condition in Figure 4 is given by inequality 7.

$$|G\ K| < |\ S\ +1/HE \qquad \forall \omega \in [0,\infty) \qquad (7)$$

E can become large at various frequencies due to the dynamics of the mechanism structure and drive train. If E is large and S is small, inequality 7 cannot be satisfied. To minimize the unmodeled dynamics, we suggest that the mechanism be designed with a minimum number of very light and rigid components. Also, K should be a low pass filter. Our previous experiments [9, 10] have shown that a 5-hertz bandwidth for K is sufficient for most maneuvers. The suggested form of K is given by equation 8.

$$K = \frac{K_o}{\tau s + 1} \qquad (8)$$

3) The effect of large sampling time

The G H K loop is a digital loop representing the information signal through the computer, and the S H loop is a continuous signal representing the power transfer to the hand controller. The computer sampling time affects the GHK loop only.

The computer sampling time determines how quickly forces sensed at the hand controller are converted to position commands. Our experiments show that since a slow computer creates a large delay between the

input force and the hand controller response, human force builds up on the hand controller. This large force then is read by the force sensor which results in movement of the hand controller with such a large velocity that it pulls the human arm forward. This reverses the direction of the contact force, f. The hand controller responds to this reverse force with a large velocity which pushes the human arm backward. This periodic motion (limit cycle instability) occurs in a very short amount of time and the motion of the hand controller becomes oscillatory. This limit cycle instability can be analyzed using describing function analysis. We suggest the use of a faster computer so the sampling time is less than 0.003 seconds.

6. EXPERIMENT

Figure 5 shows the experimental one-degree-of-freedom electrically powered hand controller. The operator's hand grasps a handle mounted on a piezoelectric force sensor. A harmonic drive is installed between the DC motor and the handle to transfer power to the handle. An encoder measures the orientation of the handle. A microcomputer is used for data acquisition and control.

Figure 5: One-Degree-of-Freedom Hand
Controller

Using the encoders for feedback, a primary stabilizing controller for the hand controller is designed to yield the widest

bandwidth for the closed-loop position transfer function, G, and yet guarantee the stability of the closed-loop positioning system in the presence of bounded unmodeled dynamics in the hand controller and harmonic drive. The development of the position controllers for the hand controller has been omitted for brevity. An experimental plot of G with the bandwidth of 10 rad/sec is given in Figure 6 .
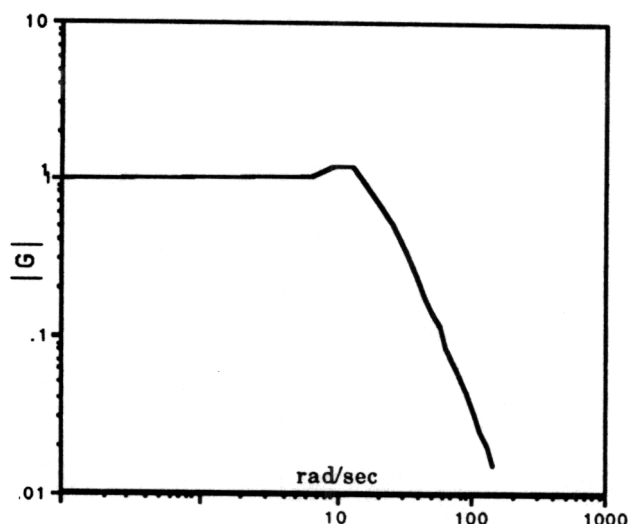

Figure 6: A closed loop position controller has been designed for the hand controller that minimizes the effects of frictional forces in the joints and in the transmission mechanism and creates a more definite dynamic behavior in the mechanism.

A human arm model was derived to verify the stability condition. The model derived for the human arm does not represent the human arm sensitivity H for all configurations of the arm; it is only an approximate and experimentally verified model of the author's arm in the neighborhood of the Figure 5 configuration. For the experiment, the author gripped the handle, and the hand controller was commanded to oscillate via sinusoidal functions. At each oscillation frequency, the operator tried to move his hand to follow the hand controller so that zero contact force was maintained between his hand and the hand controller. Since the

human arm cannot keep up with the high-frequency motion of the hand controller when trying to maintain zero contact forces, large contact forces and consequently, a large H are expected at high frequencies. Since this force is equal to the product of the hand controller acceleration and human arm inertia (Newton's Second Law), at least a second-order transfer function is expected for H at high frequencies. On the other hand, at low frequencies (in particular at DC), since the operator can follow the hand controller motion comfortably, he can always establish almost constant contact forces between his hand and the hand controller. This leads to the assumption of a constant transfer function for H at low frequencies where contact forces are small for all values of hand controller position. Based on several experiments, at various frequencies, the best estimates for the author's hand sensitivity is presented by equation 9.

$$H = (\frac{s^2}{20} + \frac{s}{5} + \frac{1}{5}) \qquad \text{lbf-ft/rad} \qquad (9)$$

Figure 7 shows the experimental values and the fitted transfer functions (equation 9) for the human arm dynamic behavior.
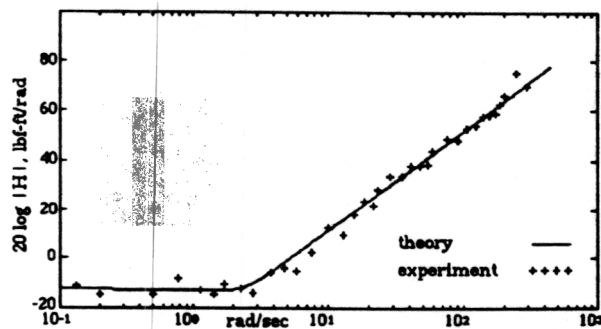

Figure 7: Human Arm Dynamic Behavior in the in the Neighborhood of the Figure 5 Configuration

22

Performance with low frequency maneuvers

A set of experiments were performed to show how the hand controller sensitivity can be shaped. In particular the objective was to make the hand controller behave like a spring: the hand controller deviation from its equilibrium position is proportional to the imposed force. Inspection of Figure 3 reveals that: $x = (S + GK)f$ where $(S + GK)$ represents the total sensitivity of the hand controller. K must be chosen such that $(S + GK)$ becomes equal to the desired sensitivity while the system stability is guaranteed. Since G (shown in Figure 6) is constant within its bandwidth, we choose K as a first order transfer function (equation 6) with a bandwidth larger than the bandwidth of G. This results in a constant overall sensitivity, $(S + GK)$, within the bandwidth of G.

Figure 8 shows f vs x for various values of K_0 when the operator pushes the hand controller uniformly. In all cases the value of K_0 (the maximum value of K for all frequencies) was less than $1/H$ satisfying the stability condition in inequality 5. The slope of each plot in Figure 7 represents the hand controller overall sensitivity or $(S + GK)$. Since S is small and G is unity within its bandwidth, the slope of each plot represents K_0.

Performance with high frequency maneuvers

In another set of experiments, the operator maneuvers the hand controller irregularly (i.e., randomly). Figure 9 shows the history of the hand controller position, x, and the human force, f, as functions of time where $K_0 = 0.2$ satisfying the stability condition in inequality 5. Irregular maneuvers create high and low frequency components in the hand controller motion. Figure 10 shows the measured force, f, versus x where the slope of 0.2 implies that the desired sensitivity of $K_0 = 0.2$ has been achieved within the system bandwidth. Figures 11 and 12 are similar to Figures 9 and 10; however, they are given for $K_0 = 0.1$. Inspection of the slope in Figure 12

verifies that desired sensitivity of $K_0 = 0.1$ has been achieved within the system bandwidth.
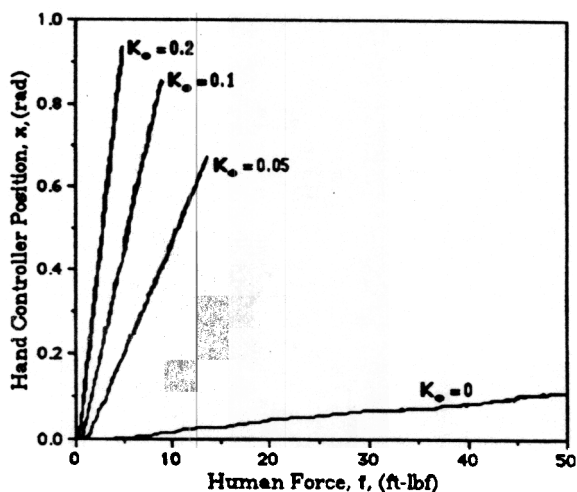

Figure 8: By Choosing K, the hand controller sensitivity function, $(S + GK)$ can be shaped as desired. The larger K_0 (the DC gain of K) is chosen to be, the more sensitive the hand controller will be in response to human forces.
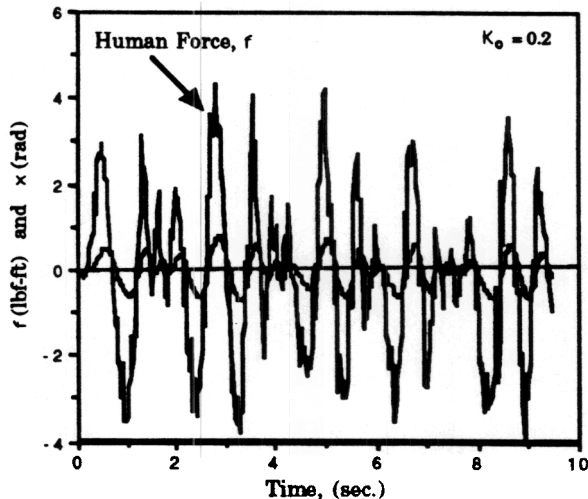

Figure 9: The time history of the human force, f, and the hand controller position, x, show that $x = 0.2\ f$ for all frequencies within the system bandwidth.
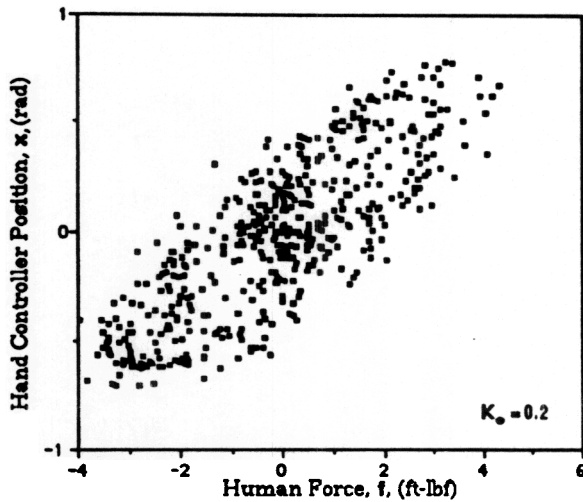
23

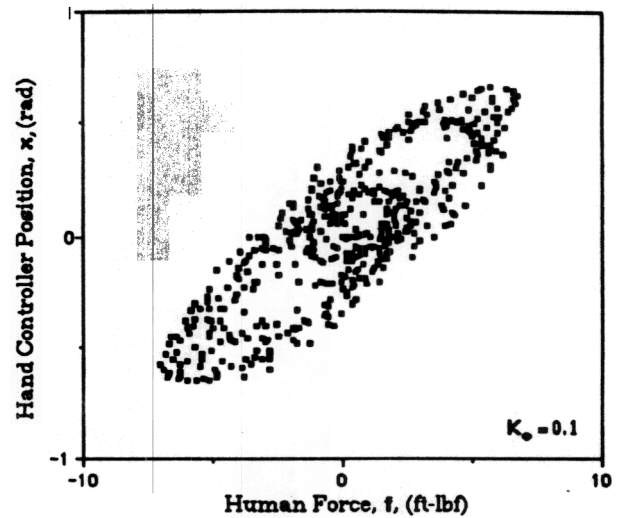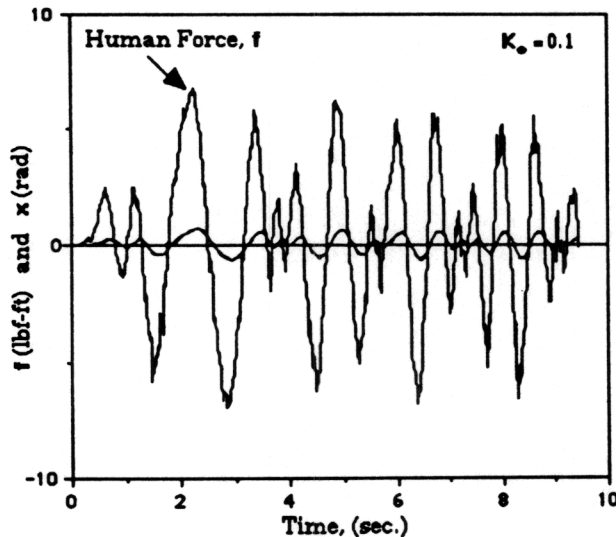Figure 10: The average slope of 0.2 reveals that x =.2 f for all frequencies within the system bandwidth.

Figure 11: The time history of the human force, f, and the hand controller position, x, show that x = 0.1 f for all frequencies within the system bandwidth.

Figure 12: The average slope of 0.1 reveals that x =.1 f for all frequencies within the system bandwidth.

Stability Condition

A set of experiments were carried out to verify the stability condition. K was chosen to be:

$$K = \frac{Ko}{(s/2 + 1)^2}$$

Figure 13 shows GK for various values of K_o ; it can be observed that for all values of K_o smaller than 5, $|GK| < |1/H|$, and satisfies the stability condition (inequality 15). Figure 14 shows the system response (x and f) when $K_o = 1$ satisfying the stability condition. Figure 15 shows the measured force, f, versus x where the slope of 1 implies that the desired sensitivity of $K_o = 1$ has been achieved within the system bandwidth. Figures 16 and 17 show the system response for $K_o = 3$. They verified that when the compensator satisfies the stability criterion, stable maneuvers, as indicated by the bounded force, occurs. Finally, figure 18 shows a maneuver where $K_o = 5$ violated the stability criterion; resulting in the unstable system.
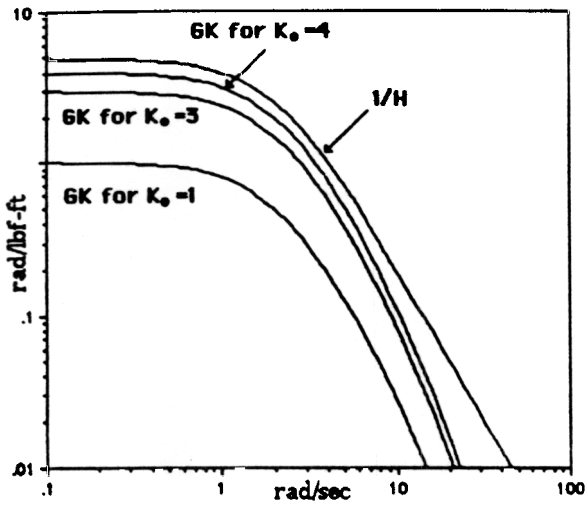
24

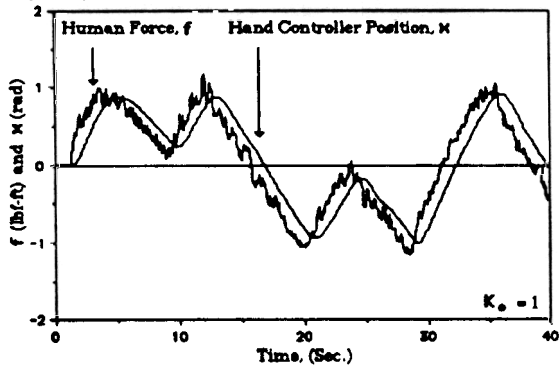Figure 13: For all values of K_o smaller than 5, $|GK|$ is smaller than $|1/H|$ satisfying 15.

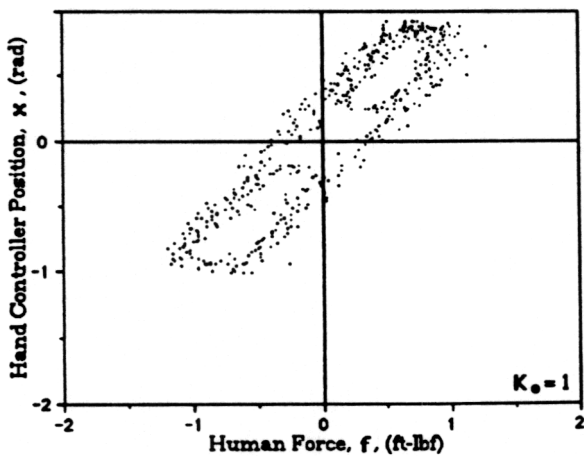Figure 14: The stable time history of the human force, f, and the hand controller position, x.

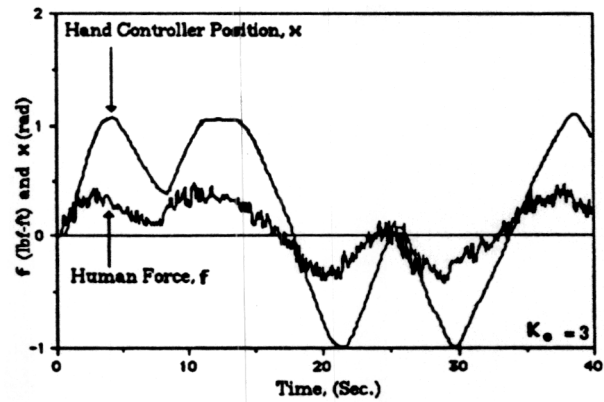Figure 15: The average slope of 1 reveals that x =1 f fwithin the system bandwidth.

Figure 16: The stable time history of the human force, f, and the hand controller position, x.

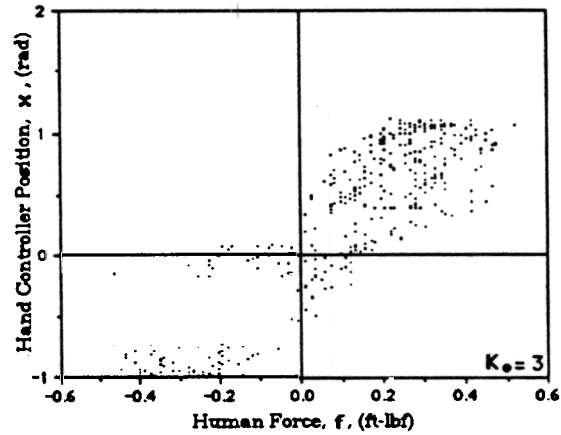

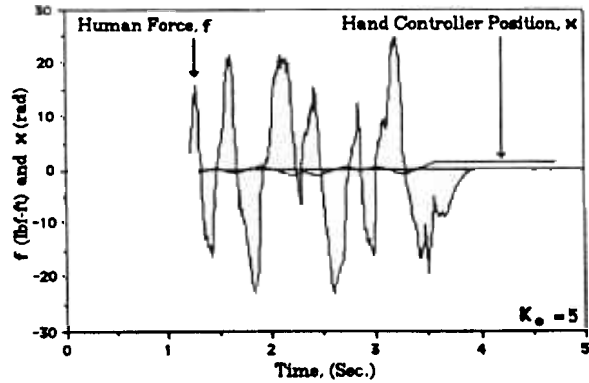Figure 17: The average slope of 3 reveals that x = 3 f for all frequencies within bandwidth.

Figure 18: The unstable time history of the human force, f, and the hand controller position, x, when the controler violates the stability condition.

7. CONCLUSION

A control architecture has been given to develop compliancy in a hand controller. It has been shown that for the stability of the hand controller and the human arm taken as a whole, there must be some compliancy either in the hand controller or in the human arm. A single-degree-of-freedom powered hand controller has been built for theoretical and experimental verification of the hand controller dynamics. A set of experiments are given to verify the system performance and stability condition.

8. REFERENCES

1) Bejczy, A. K., Handlykken, M., "Experimental Results with a Six Degree-of-Freedom Force Reflecting Hand Controller, *Proc. 17th Annual Conference on Manual Control*, Los Angeles, CA, June 1981.

2) Bejczy, A. K., Bekey, G., Lee, S. K., "Computer Control of Space Borne Teleoperators with Sensory Feedback", *IEEE Conference on Robotics and Automation*, 1985.

3) Berthoz, A., Metral, S., "Behavior of Musculra Group Subjected to a Sinusoidal and Trapezoidal Variation of Force", J. of Applied Physiol., Volume 29, pp:378-384, 1970.

4) Bruno, J. M., "The JAU-JPL Anthropomorphic Telerobot", in Proceedings of the NASA Conference on Space Telerobotics, Volume IV, January 1989.

5) Chapel, J. D., "Performance Limitations of Bilateral Force Reflection Imposed by Operator Dynamic Characteristics", in Proceedings of the NASA Conference on Space Telerobotics, Volume IV, January 1989.

6) Glusman, S. I., Landis, K. H., Dabundo, C., "Handling Qualities Evaluation of the ADOCS Primary Flight Control System", 42nd Annual Forum of the American Helicopter Society, Washington, DC, June 1986.

7) Houk, J. C., "Neural control of muscle length and tension", in: Motor control, ed. V. B. Brooks. Bethesda, MD, American Physiological Society Handbook of Physiology.

8) Jacobsen, S. C., Iversen, E. K., Knutti, D. F., Johnson, R. T., Biggers, K., "Design of the Utah/MIT Dextrous Hand", In Proceedings of the IEEE International Conference on Robotics and Automation, April 1986.

9) Kazerooni,H., "Human-Robot Interaction via the Transfer of Power and Information Signals," IEEE Transactions on Systems and Cybernetics, Vol. 20, No. 2, March 1990.

10) Kazerooni, H., Mahoney, S. M., "Dynamics and Control of Robotic Systems Worn by Humans", IEEE International Conference on Robotics and Automation, Sacramento, CA, May 1991.

11) Lehtomaki, N.A., Sandell, N.R., Athans, M., "Robustness Results in Linear-Quadratic Gaussian Based Multivariable Control Designs", IEEE Trans. on Auto. Control, Vol. AC-26, No. 1, pp. 75-92, February 1981.

12) Lindemann R., Tesar, D., "Construction and Demonstration of a 6 DOF Force Reflecting Joystick for Telerobotics", in Proceedings of the NASA Conference on Space Telerobotics, Volume IV, January 1989.

13) Lippay, A. L., King M., Kruk R. V., Morgan, M., "Helicopter Flight Control with One Hand", Canadian Aeronautiocs and Space Journal, Vo. 31, No. 4, December 1985.

14) Repperger, D. W., "Active Force Reflection Devices in Teleoperation", IEEE Control Systems, Vol. 11, No. 1, January 91.

15) Spong, M.W. and Vidyasagar, M., "Robust Nonlinear Control of Robot Manipulators," *Proc. 24th IEEE Conference on Decision and Control*, Ft. Lauderdate, Florida, 1767-1772, December 1985.

16) Stein, R. B., "What muscles variables does the nervous system control in limb movements?", J. of the behavioral and brain sciences, 1982, Volume 5, pp 535-577.

17) Szakaly, Z., Kim, W. S., Bejczy, A. K., "Force-Reflective Teleoperated System with Shared and Compliant Control Capabilities", in Proceedings of the NASA Conference on Space Telerobotics, Volume IV, January 1989.

18) Vertut, J., "Control of Master-Slave Manipulators and Force Feedback", in Proceedings of the 1977 Joint Automatic Control Conference, Page 172, San Francisco, 1977.

APPENDIX A

A simple example in Figure A1 is given here to show the that the use of transmission systems does not necessarily result in lower speed for the output shaft. The dynamic equation describing the behavior of the system can be represented as:

$$\ddot{\theta}_2 = \frac{T}{(n I_1 + I_2/n)}$$

where (I_1, R_1, θ_1) and (I_2, R_2, θ_2) represent the moments of inertia, radius and orientation of each gear $(n = R_2/R_1)$. T is the motor torque. The maximum acceleration will happen when n is chosen as:

$$n = \sqrt{I_2/I_1}$$

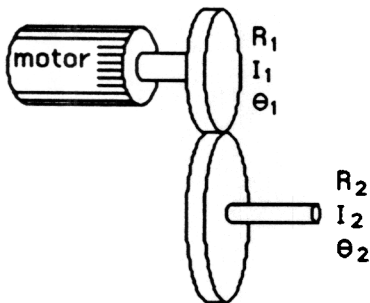For maximum acceleration, the transmission for a motor must be equal to the square root of the inertia of the output shaft to the inertia of the rotor.

Figure A1: Nondirect Drive System